Journal of the Ceramic Society of Japan 116 [3] 475-480 2008 Paper

Effect of crystallized phase on mechanical strength of hot-pressed composites of $MgO–B_2O_3–Al_2O_3$ type glass and Al_2O_3 filler

Masahide OKAMOTO, Hironori KODAMA* and Kazuo SHINOZAKI**

Production Engineering Research Laboratory, Hitachi Ltd., 292, Yoshida-cho, Totsuka-ku, Yokohama 244-0817
***Hitachi Research Laboratory, Hitachi Ltd., 7-1-1, Oomika-cho, Hitachi-shi, Ibaraki 319-1292**
****Department of Metallurgy and Ceramics Science, Tokyo Institute of Technology, 2-12-1, Oookayama, Meguro-ku, Tokyo 152-8550**

We optimized the crystallized phase for imparting high mechanical strength to a composite of $MgO–B_2O_3–Al_2O_3$ glass and Al_2O_3 filler by hot-press sintering to achieve densification at low temperature and annealing to induce crystallization. The selective crystallization of $Al_4B_2O_9$ and/or $AlBO_3$ successfully yielded a composite with high mechanical strength and low porosity. This required the use of a glass with a high Al_2O_3 content that retained its glassy character even when its entire Al_2O_3 content was converted to crystalline $Al_4B_2O_9$. The composite of $MgO–B_2O_3–Al_2O_3$ type glass and Al_2O_3 filler exhibited a higher mechanical strength than conventional borosilicate glass and Al_2O_3 filler composites, a porosity of about 1%, a low coefficient of thermal expansion, and was highly waterproof.

Key-words: Glass-ceramics, Composites, Crystallization, Hot pressing, Mechanical strength, $MgO–B_2O_3–Al_2O_3$ glass

[Received August 15, 2007; Accepted January 17, 2008]

1. Introduction

Ceramic multilayer wiring substrates are necessary for LSI (Si chip) mounted substrates of mainframe computers. These substrates must have high reliability and high heat radiation. The following characteristics are required of a ceramic material for this application: low-temperature sinterability to allow application of the Cu conductor, which is a low-electric-resistance material, a low dielectric constant for higher calculation speeds, a low coefficient of thermal expansion (CTE) to match that of Si, and a high mechanical strength to compensate for the CTE mismatch with the Cu conductor. Glass powder type materials meet these demands best. These materials can roughly be divided into two types: i) composites consisting of glass and a crystalline filler and ii) glass-ceramics. Glass generally has poor mechanical strength. Cracks are formed in it as a result of the thermal stress generated during the cooling stage after sintering. This stress is due to the mismatch between the CTE of glass and copper. Composite materials containing glass are aimed at achieving superior mechanical strength through the addition of a crystalline filler. Glass-ceramics are directed at achieving greater mechanical strength through the microcrystals that form in glass. Borosilicate glass/Al_2O_3 filler[1)-3)] and borosilicate glass/cordierite filler[4)] composites are representative examples of the former, while cordierite crystallized glass-ceramics[5)] are a representative example of the latter (**Table 1**). Composites have a low CTE but inferior mechanical strength. Glass-ceramics, on the other hand, have superior mechanical strength but a relatively high CTE. Thus, both have their own shortcomings.

The CTE of glass components can be empirically calculated. B_2O_3, SiO_2, and Al_2O_3 are representative glass components with low CTE. Thus, they are promising as glass components of the multilayer wiring substrate for mainframe computers. Among Group II oxides, MgO has the lowest CTE. These oxides do not show ionic conductivity as they have no alkali metal ion content, nor do they exhibit electronic conductivity since they have no transition metal ion content. The atomic valence transition of transition metal ions leads to electronic conductivity. As a result, these oxides also have excellent insulation properties. The main components of borosilicate glass are B_2O_3 and SiO_2, two of the three promising glass components mentioned above. The main components of cordierite crystallized glass are, again, two of the three promising components mentioned above, namely SiO_2 and Al_2O_3, plus MgO. The present study investigates this last combination (i.e., B_2O_3, Al_2O_3 and MgO glass). This type of glass is known as a crystallized glass (glass-ceramic) with Al-B-O type crystallinity, and $Mg_2B_2O_5$ is generated as a crystallized phase in the glass.[6)] In the present study, an Al_2O_3 filler was added to this glass ceramic to achieve greater mechanical strength.

Table 1. Various Glass Powder Type Materials for Substrates

Glass system	Crystalline		Reference
	Filler	Crystallized phase	
B_2O_3-SiO_2	Al_2O_3		1-3
B_2O_3-SiO_2	$2MgO·2Al_2O_3·5SiO_2$		4
MgO-Al_2O_3-SiO_2		$2MgO·2Al_2O_3·5SiO_2$	5
MgO-B_2O_3-Al_2O_3	Al_2O_3	$Al_4B_2O_9$ etc.	the present study

There have been very few reports on $MgO–B_2O_3–Al_2O_3$ glass, and the properties of this type of glass/filler composite are unknown. The CTE of $MgO–B_2O_3–Al_2O_3$ type glass is known to be $4–6\times10^{-6}$/°C,[7)] which is relatively low. The glass-forming region in the $MgO–B_2O_3–Al_2O_3$ system is outlined in **Fig. 1**.[8)-10)] B_2O_3 is a glass former, Al_2O_3 is a network former, and MgO is a modifier. The glass transition temperature[11),12)] and the softening temperature[13),14)] of the compositions in the glass-forming region of the $MgO–B_2O_3–Al_2O_3$ system were reported to be 637–649°C and 735°C,

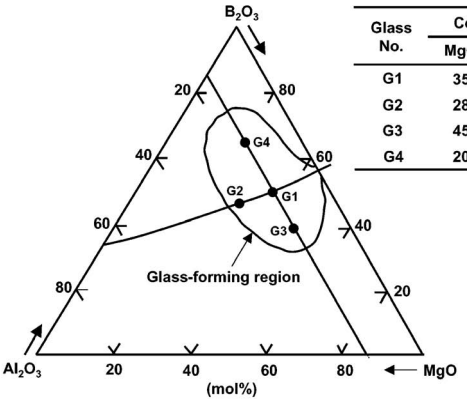

Glass No.	Composition (mol%)		
	MgO	B_2O_3	Al_2O_3
G1	35	50	15
G2	28	47	25
G3	45	40	15
G4	20	65	15

Fig. 1. Glass-forming region in the $MgO–B_2O_3–Al_2O_3$ system and compositions examined.

respectively. It is too difficult to achieve densification of this composite by pressure-less sintering, as we will describe in the beginning of Section 3. Thus, we presumed that most important for increasing the strength was the optimization of the crystallized phase in this composite of glass and Al_2O_3 filler, and employed annealing for crystallization after hot pressing at low temperature for densification. We will attempt to fabricate this material by pressure-less sintering in our next report.[15]

2. Experimental procedure

High-grade reagents of MgO, H_3BO_3, and Al_2O_3 (Wako Pure Chemical Industries, Ltd.) were used as raw material powder for the glass. AL-45-A (Showa Denko K.K.) was used as the Al_2O_3 filler. This is an α-Al_2O_3 powder with a mean particle diameter of 1.1 μm. We performed preliminary tests on the 1.1-μm powder and a 2.1-μm powder as Al_2O_3 filler. We selected the 1.1-μm powder because it yielded a composite with a higher mechanical strength than the 2.1-μm powder. The reason is thought to be the following. Fine powder is better from the viewpoint of strengthening by particle deflocculation. On the other hand, when the Al_2O_3 filler is too fine, it disappears because it reacts with the glass; as a result, the effect of the filler (high strengthening) also disappears. Thus, we selected the 1.1-μm powder. The glass compositions we investigated are listed in Fig. 1. The curve, on which compositions G1 and G2 lie, represents those compositions that retain their glassy state even when all Al_2O_3 components in the glass crystallize into $Al_4B_2O_9$. $Al_4B_2O_9$ has an Al-B-O type crystal structure. Composition G1 is located at almost the center of the glass-forming region. The Al_2O_3 content of G1 is 15 mol%. G2, which has a higher Al_2O_3 content, is located on the edge of the glass-forming region. G3 and G4 have the same Al_2O_3 content as G1, namely 15 mol%. G3 and G4 are compositions that differ greatly from G1 in terms of the MgO/B_2O_3 ratio in the glass-forming region. Compositions having Al_2O_3 contents lower than that of G1 on the curve were not investigated in the present work because glass of such low Al_2O_3 content mostly reacts with the Al_2O_3 filler, as a result of which most of the Al_2O_3 filler disappears. We reasoned that it would be too difficult to increase the strength of the composites if we were to use those compositions.

The procedure we used to prepare the glass powder is explained below. The prescribed amount of raw material powder for the glass was melted and stirred well in a high-purity Al_2O_3 crucible at 1400–1450°C. The molten glass was rapidly cooled upon being transferred from the crucible onto a metal plate to obtain a glass block. The glass powder for hot-press firing was obtained by crushing the block in an Al_2O_3 mortar into a coarse powder, about 2 mm in diameter, and further crushing it mechanically into a-100 mesh powder. The sample preparation procedure is schematized below. Glass powder and Al_2O_3 filler powder (total 0.06 kg) were mixed with distilled water (1.3×10^{-4} m^3) to form uniformly distributed and agate balls (15 20-mm-diameter balls and 30 15-mm-diameter balls) and ball-milled in a 5×10^{-4} m^3 polyethylene pot for 24 h. The ball mill was operated at 70 rpm. The content of the Al_2O_3 filler powder was fixed at 25 vol% of the total glass powder and Al_2O_3 filler powder. We aimed for a CTE of about 4×10^{-6}/K for the composite by considering its difference from the CTE of Cu. We calculated that a 25 vol% addition of Al_2O_3 filler is necessary for this objective. After ball milling, the slurry was dried at 120°C for 10 h in air and the dried cake was broken up in an Al_2O_3 mortar. The resultant powder was granulated to a-32 mesh powder and uniaxially pressed into a 60-mm-diameter, 10-mm-thick disk using a pressure of 34.3 MPa. No organic binder was added to the green compact during this forming process. The hot-pressed sample was obtained by hot-press firing this compact under a pressure of 29.4 MPa in a 111-kPa N_2 atmosphere. The heating rate was 300°C/h. The furnace temperature was kept at the sintering end temperature for 1 h, and then the pressure was released, and the sample was cooled naturally. The sinter-shrink start and end temperatures could be obtained from the displacement curve for the press mold during hot pressing. We used a FVPHP-15 (Fuji Dempa Kogyo Co., Ltd.) as the hot-press furnace under a high-pressure atmosphere. The hot-pressed sample was cut in half. One of these halves was annealed at 950°C for 1 h in air to enable crystallization. The heating rate was 200°C/h. The sample was cooled naturally.

A Rigaku (Japan) NC-DM dilatometer was used to measure the pressure-less sintering curve of the composites. The green compact was sintered for 5 min at 1000°C in air. The heating and cooling rates were 3°C/min and 5°C/min, respectively. The density of the sample was measured by the Archimedes method. Its mechanical strength was measured through four-point bending tests. The widths of the upper and lower spans were 10 and 30 mm, respectively. The cross-head speed was set at 0.5 mm/min. We used an Autograph DSS-5000 (Shimadzu Co.) as the test fixture. Five test pieces were used for measurement. The size and shape of the test pieces for the bending test conformed to JIS-R-1601. The microstructure of the samples was characterized by a scanning electron microscope (SEM S-570, Hitachi, Japan). Since the samples were insulating, they were coated with Au + Pd prior to SEM characterization. We analyzed the crystal phase in the samples using powder X-ray diffraction. A wide-angle X-ray diffraction device (Rotaflex, Rigaku) was used for measurement. The Cu target was irradiated with X-rays under a voltage of 40 kV and a current of 100 mA. The crystal phase was identified by using a Powder Diffraction File and American Society for Testing Materials (ASTM) cards. The CTE was measured with a thermo-mechanical analyzer (2F-TMA, Rigaku) at a heating rate of 3°C/min (RT-200°C) in air. The test pieces for the CTE

measurement were prepared by cutting the sample into $3 \times 3 \times 30$ mm sections. The samples' durability in water was measured on the basis of the change in the weight of the test pieces before and after a 2 h immersion in water at 70°C. Before immersion, the test pieces were ultrasonicated in acetone for 5 min. The test pieces for measuring durability in water were made by cutting the sample into $3 \times 4 \times 8$ mm sections and polishing all surfaces to a mirror finish. This is the standard method for durability testing of ceramic materials for the multilayer wiring substrate of mainframe computers.

3. Results and discussion

3.1 Density and microstructure of sintered composite

All the G1–G4 glass blocks prepared were colorless and transparent. Their respective densities were 2.53, 2.53, 2.60, and 2.38×10^3 kg/m^3. The glass that contained a large amount of B_2O_3 had a relatively low density because B_2O_3 has a low density. The glass densities in this work corresponded almost exactly to those in previous works.[10),11),16)–18)] We see the dilatometric pressure-less sintering curve and DTA trace of a composite of 75 vol% G2 glass and 25 vol% Al_2O_3 filler in **Fig. 2**. The inset shows a room-temperature XRD pattern obtained after firing and an SEM micrograph of an at 1000°C fired glass composite fracture surface. We used a glass powder with an average particle size of 2.4 μm, which was sufficiently fine for pressure-less sintering. There was a large exothermic peak around 760°C. Our XRD analysis results revealed that this peak corresponded to $Al_4B_2O_9$ crystallization. The firing shrinkage seemed to cease owing to this crystallization. The amount of glass, which has liquidity and low viscosity, decreased because of the crystallization, and this hindered sintering after crystallization. There were many pores in this composite's fracture surface and its sinterability was low. Thus, we annealed the composite of glass and Al_2O_3 filler to achieve crystallization after hot pressing at low temperature for densification. This method allowed us to completely isolate the sintering (densification) and crystallization processes.

The firing shrinkage start and end temperatures for hot-pressing of the composites of G1–G4 and Al_2O_3 filler and the densities after hot-pressing are given in **Fig. 3**. The shrinkage end temperature for all composites was 640°C. The shrinkage end temperature strongly depends on the amount of Al_2O_3 filler, which impedes the sintering of glass powder.[19)] There are no differences in shrinkage end temperature because the amount of Al_2O_3 filler added was the same for all samples. The shrinkage start temperatures ranged between 520°C and 540°C range. A lower glass softening temperature is thought to decrease the shrinkage start temperature. There was no crystallization in any of the samples and no crystallinity besides the Al_2O_3 filler because the samples were hot-pressed at a temperature lower than the crystallization temperature. The XRD pattern of G2 composite obtained after hot pressing is shown in **Fig. 4**. as an example. Moreover, it was found that there was hardly any reaction between the glass and the Al_2O_3 filler. Thus, we calculated the theoretical density of each composite from the density of the glasses mentioned above and the density of Al_2O_3. The measured densities and the relative densities of the composites are listed in Fig. 3. The relative densities of glass/filler compounds, with the exception of G4, were almost 100%. SEM images of the polished surfaces of hot-pressed composites of G1–G4 and Al_2O_3 filler are shown in **Fig. 5**. The G4 glass composite, whose relative density was slightly low, had some pores. The other composites, on the other hand, were mostly dense and showed few pores.

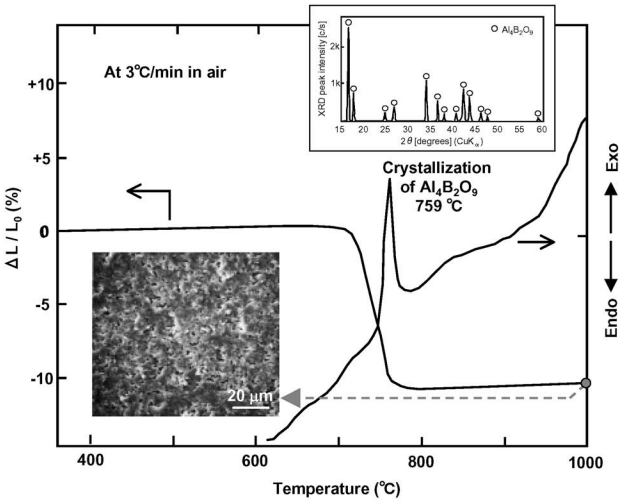

Fig. 2. Dilatometric sintering curve and DTA trace of G2 composite, sintered in air at 3°C/min. The inset shows a room-temperature XRD pattern obtained after firing and a SEM micrograph of an at 1000°C fired glass composite fracture surface.

Sample	Shrink start and end temperatures for hot-press firing (°C) 500 550 600 650 700	Density (10^3 kg/m^3)	Relative density (%)
G1 composite*	start – end	2.89	100
G2 composite*	–	2.88	99.7
G3 composite*	–	2.97	100
G4 composite*	–	2.60	94.0

* 75 vol% glass and 25 vol% Al_2O_3 filler

Fig. 3. Shrink start and end temperatures for hot-press sintering of composite of 75 vol% $MgO–B_2O_3–Al_2O_3$ type glass and 25 vol% Al_2O_3 filler, and the density and relative density of the hot-pressed composite.

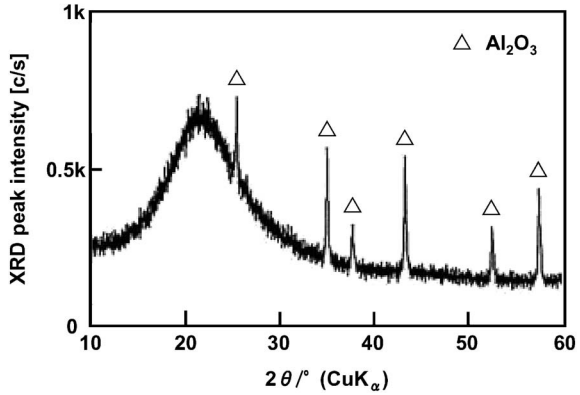

Fig. 4. XRD pattern of G2 composite obtained after hot pressing.

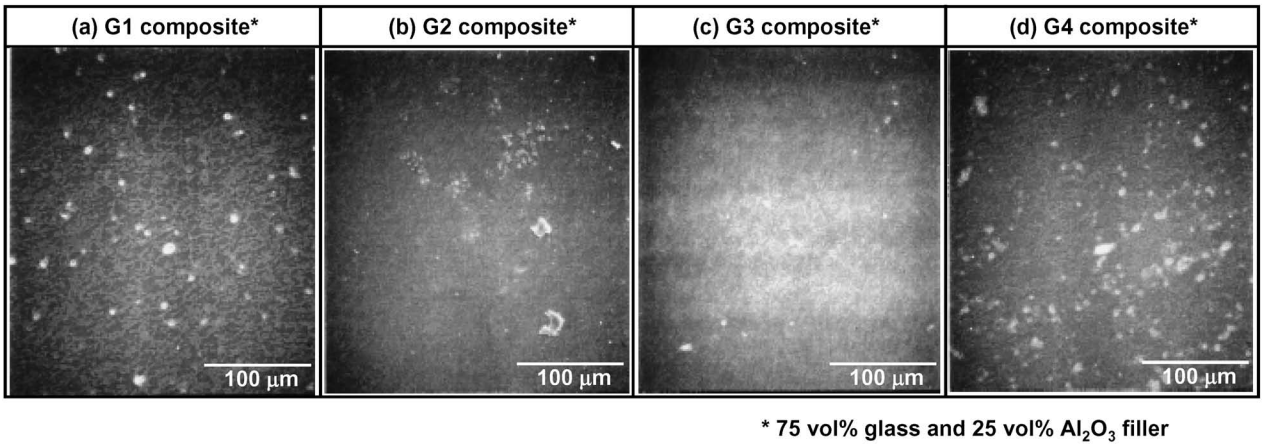

Fig. 5. SEM micrographs of the polished surface of a hot-pressed composite of 75 vol% $MgO–B_2O_3–Al_2O_3$ type glass and 25 vol% Al_2O_3 filler.

Sample	Density (10^3 kg/m^3)	Four-point bending strength (MPa)*2
G1 composite*1	2.65	
G2 composite*1	2.71	
G3 composite*1	2.89	
G4 composite*1	2.30	

100 150 200 250 300

*1 75 vol% glass and 25 vol% Al_2O_3 filler, hot-pressed + annealed
*2 No. of test pieces: 5

Fig. 6. Density and four-point bending strength of a hot-pressed and annealed composite of 75 vol% $MgO–B_2O_3–Al_2O_3$ type glass and 25 vol% Al_2O_3 filler.

3.2 Optimization of crystals formed in composites for high mechanical strength

In the next stage, the hot-pressed glass/Al_2O_3 filler composites were annealed for crystallization. The density and four-point bending strength of hot-pressed and annealed composites of G1–G4 and Al_2O_3 filler are outlined in **Fig. 6**. Composites of G1 and G2 still had a relatively high strength (250 MPa or more) after annealing. The strength of the G4 composite, in particular, was greatly reduced to 150 MPa. The density of all composites decreased upon annealing. SEM images of polished surfaces of hot-pressed and annealed composites of G1–G4 and Al_2O_3 filler are shown in **Fig. 7**. The glass composite of G2 was the strongest and had low porosity while that of G4 was the weakest and had high porosity. We estimated the porosity in the samples from SEM micrographs. The pore percentage for composites of G1, G2, G3, and G4 was about 1, 0, 1, and 5 vol%, respectively. We calculated the theoretical density of all composites from these values. The amount of residual Al_2O_3 filler in all composites was estimated from their theoretical density, the density of the glass, and the density of Al_2O_3. The amount of residual Al_2O_3 filler in the G1, G2, G3, and G4 composites was about 11, 13, 24, and 14 vol%, starting with an initial amount of 25 vol%. The amount of Al_2O_3 filler decreased because it reacted with the glass during annealing. Here, we assumed that there were no changes in the glass due to the reaction between the glass and Al_2O_3 filler. However, the density of glass is known to actually increase by 0.0025–0.009×10^3 kg/m^3 when 1 mol of Al_2O_3 merges into these glasses.[10),17),18)] Thus, we presumed that the actual amount of residual Al_2O_3 filler would be slightly less than the value calculated previously. The crystalline phases of the annealed samples are listed in **Table 2**. Clearly, a certain amount of Al_2O_3 filler remained in all annealed samples. However, with the exception of the G3 composite, the amount of Al_2O_3 filler decreased upon annealing. The behavior of the peak intensity of Al_2O_3 corresponded well to the amount of residual Al_2O_3 filler calculated previously. Moreover, there was a great deal of $Al_4B_2O_9$ crystallization in all annealed samples, and $AlBO_3$, $Al_{18}B_4O_{33}$, $Mg_2B_2O_5$, and MgB_4O_7 crystallization in some. The annealed G2 composite only contained $Al_4B_2O_9$ and $AlBO_3$ and not contained Mg–B–O crystalline and $Al_{18}B_4O_{33}$ and had few voids and outstanding strength.

We speculated that there were three possible reasons for the annealing-induced density decrease:

(1) The Al_2O_3 filler reacted and merged with the glass; as a result, the Al_2O_3 filler content in the composite decreased.

(2) There were originally minute pores between the Al_2O_3 filler particles in the composites because the composites contained Al_2O_3 filler. These pores grew during annealing because the CTE for the *a*-axis of α-Al_2O_3 is different from that for the *c*-axis.

(3) Pores and cracks occurred in the composite due to crystallization during annealing.

It is thought that the order of mechanical strength and density of the annealed samples were as follows. The density of the mother glasses ranged from 2.38 to 2.53. The density of $AlBO_3 = Al_2O_3–B_2O_3$, $Al_4B_2O_9 = 2Al_2O_3–B_2O_3$ and $Al_{18}B_4O_{33} = 9Al_2O_3–2B_2O_3$ is 3.22, 3.47and 3.70, respectively. The smaller Al_2O_3/B_2O_3 ratio of crystal, the density of crystal is more close to that of the mother glass. Therefore, the generation of $Al_4B_2O_9$ and/or $AlBO_3$ did not lead to a great change in volume and little pore and crack occured in the composites. However, there were great differences between Mg–B–O crystalline as well as $Al_{18}B_4O_{33}$ densities and that of the mother glass. The volume of the crystallized portion may have contracted considerably, resulting in the formation of pores and cracks. It is necessary to selectively

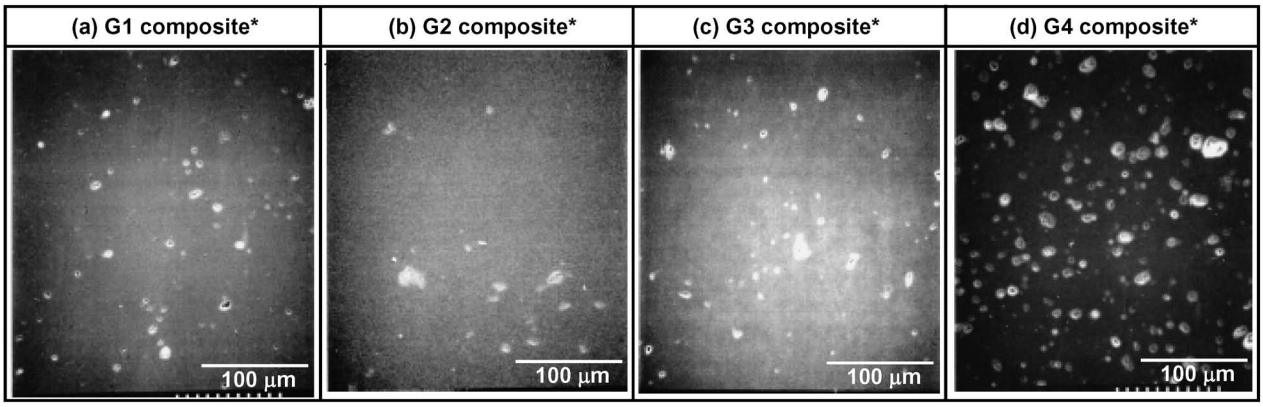

Fig. 7. SEM micrographs of the polished surface of a hot-pressed and annealed composite of 75 vol% $MgO–B_2O_3–Al_2O_3$ type glass and 25 vol% Al_2O_3 filler.

Table 2. Crystalline Phase of Annealed Composites of 75 vol% $MgO–B_2O_3–Al_2O_3$ Type Glass and 25 vol% of Al_2O_3 Filler

Sample	Crystalline phase					
	Filler	Crystallized phase				
	Al_2O_3	$AlBO_3$	$Al_4B_2O_9$	$Al_{18}B_4O_{33}$	$Mg_2B_2O_5$	MgB_4O_7
G1 composite*1	M	W	S		M	
G2 composite*1	M	W	S			
G3 composite*1	S		S		M	
G4 composite*1	M	W	S	W	M	W

*1 75 vol% glass and 25 vol% Al_2O_3 filler

* XRD peak intensity S: Strong M: Medium W: Weak

$AlBO_3 = Al_2O_3 \cdot B_2O_3$ $Al_4B_2O_9 = 2Al_2O_3 \cdot B_2O_3$ $Al_{18}B_4O_{33} = 9Al_2O_3 \cdot 2B_2O_3$

$Mg_2B_2O_5 = 2MgO \cdot B_2O_3$ $MgB_4O_7 = MgO \cdot 2B_2O_3$

Table 3. Various Properties of the 75 vol% G2 Glass/25 vol% Al_2O_3 Filler Composite*1

Properties	Value	Required value
Density ($\times 10^3$ kg/m^3)	2.71	—
Bending strength (MPa)	263	> 200
Thermal coefficient of expansion ($\times 10^{-6}$/K) [RT-200°C]	4.1	3.0 (Si)
Dielectric constant at 1 MHz	(6.0)*2	< 6
Porosity (%)	~ 1	< 1
Water-proof [weight decrease rate] (%)	0.11	0.06 (Al_2O_3)
Crystalline phase	Al_2O_3 (filler), $Al_4B_2O_9$, $AlBO_3$	—

*1 Hot-pressed at 640°C, 29.4 MPa for 1 h in N_2 + Annealed at 950°C for 1 h in air

*2 Pressure-less sintered at 1000°C for 1 h in air

crystallize $Al_4B_2O_9$ and/or $AlBO_3$ and not to crystallize Mg–B–O crystalline and $Al_{18}B_4O_{33}$ to maintain strength and low porosity after annealing. The crystals formed may have had a greater effect than the Al_2O_3 filler on the mechanical strength of the composites because the G3 glass composite with the highest residual Al_2O_3 filler content was not the strongest.

3.3 Various properties of a composite in which the crystallization is optimized

Table 3 lists the properties of the annealed composite of G2 and Al_2O_3 filler, which has the highest strength of all the annealed samples (263 MPa). As the decrease in weight in this sample is 0.11%, which is nearly equal to that in the composite of borosilicate glass and Al_2O_3 filler (0.03%) and Al_2O_3 (0.06%) in the water-durability test, this sample has excellent waterproof properties. This decrease in weight is smaller than that for the same type of glass in a previous study[20] because the sample in the present study contained 25 vol% Al_2O_3 filler. The CTE of this sample was relatively low: 4.1×10^{-6}/K (RT-200°C). The CTE of G2 glass was 3.2×10^{-6}/K. The porosity in this sample was about 1%, and its density was 2.71×10^3 kg/m^3. The CTE of this sample was nearly equal to that of a borosilicate glass/Al_2O_3 filler[1)-3)] composite (4.0×10^{-6}/K), and its strength was higher than that of a borosilicate glass/Al_2O_3 filler[1)-3)] composite (196 MPa). The dielectric constant of this composite pressure-less sintered was relatively low: 6.0 at 1 MHz.[15] Thus, this composite is suitable as the ceramic material for a multilayer wiring substrate with high-density Cu wiring. A future goal is to render this composite capable of being pressure-less sintered.

4. Conclusions

We optimized the crystallization process to fabricate a high-mechanical-strength composite of $MgO–B_2O_3–Al_2O_3$ glass and Al_2O_3 filler as a ceramic substrate material by low-temperature sintering. We employed a process that consisted of densification at low temperature by hot-press firing and crystallization by pressure-less annealing. Thus, we completely isolated the sintering and crystallization processes and eliminated porosity, which has an adverse effect on strength. We investigated the relationship between the crystallization and the strength of the composites and found:

(1) A glass composition of $Al_4B_2O_9$ and/or $AlBO_3$ selectively crystallized and Mg–B–O crystalline and $Al_{18}B_4O_{33}$ not crystallized in a composite of glass and Al_2O_3 filler was necessary to achieve a high mechanical strength and low porosity. This required the use of a glass that remained a glass even when all Al_2O_3 components in the glass crystallized into $Al_4B_2O_9$, more specifically, a glass with a high Al_2O_3 content.

(2) A composite of 75 vol% $MgO–B_2O_3–Al_2O_3$ type glass (MgO: 28 mol%, B_2O_3: 47 mol%, Al_2O_3: 25 mol%) and 25 vol% Al_2O_3 filler had a four-point bending strength

of 263 MPa, a porosity of about 1%, a CTE of 4.1×10^{-6}/K in the RT–200°C range, and excellent waterproof properties, after hot-press firing at 640°C for 1 h and annealing at 950°C for 1 h. This composite had a higher strength than the conventional composite, and is suitable for use as a ceramic material for a multilayer wiring substrate with high-density Cu wiring.

References

1) K. Niwa et al., *Advanced Ceramic Materials*, 2, No. 4, 832–835 (1987).
2) K. Niwa et al., *Advances in Ceramics*, 19, 41–47 (1987).
3) K. Niwa et al., *Advances in Ceramics*, 26, 323–337 (1989).
4) Y. Shimada et al., *Electron. Compon. Conf.*, 33, 314–319 (1983).
5) S. H. Kinckerbocker, A. H. Kumar and L. W. Herron, *Am. Ceram. Soc. Bull.*, 72, No. 1, 90–95 (1993).
6) R. Dupree, D. Holland, and D. S. Williams, *Physics and Chemistry of Glasses*, 26, No. 2, 50–52 (1985).
7) O. V. Mazurin, M. V. Streltsina and T. P. Shvaiko-Shvaikovskaya, "Physical Sciences Data 15. Handbook of Glass Data, Part D" (1991) pp. 213–215 and 217.
8) D. M. Krol et al., *J. Luminescence*, 37, 293–302 (1987).
9) M. Imaoka, *Rep. Inst. Ind. Sci. Univ. Tokyo*, 6, 127–183 (1957).
10) J. Fukunaga, R. Ota, M, Shiroyama and N. Yoshida, *J. Chemical Society of Japan*, 12, 1971–1976 (1988).
11) Y. B. Saddeek, H. F. M. Mohamed and M. A. Azooz, *Phys. Stat. Sol. (a)*, 201, No. 9, 2053–2062 (2004).
12) O. V. Mazurin, M. V. Streltsina and T. P. Shvaiko-Shvaikovskaya, "Physical Sciences Data 15. Handbook of Glass Data, Part D"(1991) 217.
13) A. Abou-El-Azm and H. A. El-Batal, *Physics and Chemistry of Glasses*, 10, No. 4, 159–163 (1969).
14) N. A. Ghoneim and H. A. El Batal, *J. Non-Cryst. Solids*, 55, 343–351 (1983).
15) M. Okamoto, H. Kodama and K. Shinozaki, *J. Am. Ceram. Soc.*, accepted for publication (JACERS-23183).
16) S. Inaba, S. Oda and K. Morinaga, *J. Japan Inst. Metals*, 65, No. 8, 680–687 (2001).
17) O. V. Mazurin, M. V. Streltsina and T. P. Shvaiko-Shvaikovskaya, "Physical Sciences Data 15. Handbook of Glass Data, Part D"(1991) pp. 202–203 and 206.
18) O. V. Mazurin, M. V. Streltsina and T. P. Shvaiko-Shvaikovskaya, "Physical Sciences Data 15. Handbook of Glass Data, Part E"(1993) p. 618.
19) N. Kamehara and K. Niwa, *Hybrids*, 2, No. 4, 9–13 (1986).
20) O. V. Mazurin, M. V. Streltsina and T. P. Shvaiko-Shvaikovskaya, "Physical Sciences Data 15. Handbook of Glass Data" (1991) p. 246.